AAC Journals.ASM.org

Antibacterial Properties of an Oligo-Acyl-Lysyl Hexamer Targeting Gram-Negative Species

Fadia Zaknoon,[a] Keren Goldberg,[a] Hadar Sarig,[a] Raquel F. Epand,[b] Richard M. Epand,[b] and Amram Mor[a]

Department of Biotechnology & Food Engineering, Technion—Israel Institute of Technology, Haifa, Israel,[a] and Department of Biochemistry and Biomedical Sciences, McMaster University, Hamilton, Ontario, Canada[b]

Toward developing new tools for fighting resistance to antibiotics, we investigated the antibacterial properties of a new decanoyl-based oligo-acyl-lysyl (OAK) hexamer, aminododecanoyl-lysyl-[aminodecanoyl-lysyl]$_5$ (α_{12}-5α_{10}). The OAK exhibited preferential activity against Gram-negative bacteria (GNB), as determined using 36 strains, including diverse species, with an MIC$_{90}$ of 6.2 μM. The OAK's bactericidal mode of action was associated with rapid membrane depolarization and cell permeabilization, suggesting that the inner membrane was the primary target, whereas the observed binding affinity to lipoteichoic acid suggested that inefficacy against Gram-positive species resulted from a cell wall interaction preventing α_{12}-5α_{10} from reaching internal targets. Interestingly, perturbation of the inner membrane structure and function was preserved at sub-MIC values. This prompted us to assess the OAK's effect on the proton motive force-dependent efflux pump AcrAB-TolC, implicated in the low sensitivity of GNB to various antibiotics, including erythromycin. We found that under sub-MIC conditions, wild-type *Escherichia coli* was significantly more sensitive to erythromycin (the MIC dropped by >10-fold), unlike its *acr*-deletion mutant. Collectively, the data suggest a useful approach for treating GNB infections through overcoming antibiotic efflux.

Host defense peptides (HDPs) are part of the innate immune system, providing a first line of defense against a wide range of invading pathogens (3, 28). Current efforts to address the shortcomings of HDPs have focused on biomimetic strategies (6, 11, 12, 22). Several short synthetic oligomers such as polymethacrylate (5), arylamide foldamers (1, 2), and oligo-acyl-lysyls (OAKs) (9) have attracted particular attention due to their lower cost and rapid structural optimization capabilities. Although a number of compounds that demonstrate broad-spectrum antimicrobial activities *in vitro* have been identified, robust/safe *in vivo* activity has been a great challenge for most published peptidomimetics. Clearly, to generate efficient HDP mimics, the mechanism of action of this class of molecules needs to be better understood. Many of the details regarding the mechanism of limiting bacterial viability—which can vary widely for different sequences—have yet to be elucidated or are widely debated. Nevertheless, a rich variety of mechanistic studies has emphasized the importance of physicochemical attributes—such as charge and hydrophobicity—for potency and selectivity. In this respect, simple mimics of HDPs might be helpful in improving understanding of critical mechanistic steps. Among the classes of HDP mimics proposed, OAKs are quite interesting due to their remarkable simplicity.

OAKs are composed of a small number of building blocks referred to as α_i (acyl-lysyl) or β_i (lysyl-acyl-lysyl) subunits (8, 13, 14), where *i* specifies the number of carbons in the acyl moiety (Fig. 1). Such a design allows systematic and gradual variations of charge and hydrophobicity and the dissection of their individual importance. Available data on the structure-activity relationships (SARs) of OAKs suggest their usefulness in improving understanding of the molecular basis for potency and selectivity (13, 17, 18). Recent designs have, moreover, shown potential for systemic efficacy (4, 19, 27), including upon coencapsulation with antibiotics in lipid vesicles (7, 20). Among these, decanoyl-based OAKs were suggested to represent an efficient platform for the design of improved antibacterial compounds, as illustrated with the broad-spectrum bactericidal sequence dodecanoyl-lysyl-[lysyl-aminodecanoyl-lysyl]$_3$ (C_{12}K-3β_{10}), which demonstrated potential for systemic treatment of *Staphylococcus aureus* infection in mice (8). To follow up on these observations, we designed and tested a new series of decanoyl-based derivatives. A preliminary screen revealed an active sequence, aminododecanoyl-lysyl-[aminodecanoyl-lysyl]$_5$ (α_{12}-5α_{10}), having a high degree of analogy with C_{12}K-3β_{10}, where the major distinctive structural feature was a different spread of the total positive charge (+7) along the peptide backbone (Fig. 1). Here, we describe the biophysical properties of α_{12}-5α_{10}, emphasizing the importance of charge distribution in selective activity over Gram-negative bacteria (GNB). In addition, we provide evidence for the ability of this new OAK derivative to alter crucial functions of the cytoplasmic membrane at subinhibitory concentrations and the consequences on antibiotic efflux.

MATERIALS AND METHODS

Peptide synthesis. The OAKs were synthesized by the solid-phase method by applying 9-fluorenylmethyloxy carbonyl (Fmoc) active ester chemistry (model 433A; Applied Biosystems) essentially as described previously (14). The crude compounds were purified to chromatographic homogeneity (>95% purity) by reverse-phase high-performance liquid chromatography (HPLC) with a chromatograph equipped with a mass spectrometer (MS; Alliance-ZQ; Waters). HPLC runs were performed on a C_{18} column (Vydac) with a linear gradient of acetonitrile in water (1%/min); both solvents contained 0.1% trifluoroacetic acid. The purified compounds were subjected to MS analysis in order to confirm their composition and stocked as lyophilized powders at −20°C. Prior to testing, fresh

Received 14 March 2012 Returned for modification 25 April 2012
Accepted 21 June 2012
Published ahead of print 2 July 2012
Address correspondence to Amram Mor, amor@tx.technion.ac.il.
Supplemental material for this article may be found at http://aac.asm.org/.

doi:10.1128/AAC.00511-12

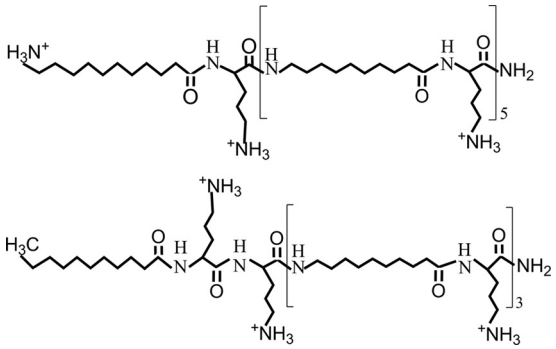

FIG 1 Molecular structure of two OAK analogs bearing 7 positive charges. The upper structure is composed of α_{12}-5α_{10}. The lower structure is of a previously investigated sequence (8) composed of C_{12}K-3β_{10}.

solutions were prepared in water (Milli-Q; Millipore), briefly vortexed, sonicated, centrifuged, and then diluted in the appropriate medium.

Bacteria used. The Gram-negative species tested included *Escherichia coli* (strains AG100, AG100A, AG100/KS, AB301, N281, ATCC 35218, ATCC 43894, and ATCC 25922 and clinical isolates 14182, 14384, U16327, U16287, U16223, U16377, U16328, U16147, U16325-2, U16329, U14215, U16229, U16228, and U16302), *Pseudomonas aeruginosa* (ATCC 9027 and ATCC 11662 and clinical isolates 1278, 1277, 1275, 12777, 8732, U13216, and 11662), *Salmonella enterica* serovar Typhimurium (ATCC 14028), *Salmonella enterica* serovar Choleraesuis (ATCC 7308), and *Klebsiella pneumoniae* (clinical isolates 1286, 1331, and 1287).

The Gram-positive species were *Staphylococcus aureus* (ATCC 25923, ATCC 29213, and ATCC 43300 and clinical isolates 15903 [a methicillin-resistant *S. aureus* {MRSA} strain], 15852 [MRSA], 15819 [a methicillin-susceptible *S. aureus* {MSSA} strain], 15877 [MRSA]), *Staphylococcus epidermidis* (ATCC 12228), *Staphylococcus xylosus* (ATCC 29971), *Enterococcus faecalis* (ATCC 29212), *Enterococcus faecium* (ATCC 35667), *Streptococcus agalactiae* (ATCC 27956), *Streptococcus bovis* (ATCC 9809), *Streptococcus pyogenes* (ATCC 19615), *Bacillus cereus* (ATCC 11778), *Listeria welshimeri* (ATCC 35897), *Listeria ivanovii* (ATCC 19119), *Listeria grayi* (ATCC 19120), and *Listeria seeligeri* (ATCC 35967).

Antibacterial assays. The MICs were determined using a microdilution assay. Bacteria were grown overnight in the suitable medium broth (brain heart infusion or LB broth) and diluted 10,000-fold in growth medium. In sterilized 96-well plates, 100 μl of growth medium containing bacteria (1×10^6 CFU/ml) was added to 100 μl of culture medium containing the test compound in serial 2-fold dilutions. Inhibition of proliferation was determined by optical density measurements (620 nm) after incubation overnight at 37°C (14).

Chemosensitization was assessed similarly, except that bacteria were incubated with a mixture of OAK and antibiotic.

The bactericidal kinetics were determined in test tubes in a final volume of 1 ml, as follows: 100 μl of suspension containing bacteria at 10^6 CFU/ml in culture medium was added to 900 μl of culture medium containing zero or various concentrations of OAK, antibiotic, or a mixture of OAK and antibiotic in serial 2-fold dilutions. After 0, 30, 60, 120, 180, and 360 min of exposure to the test compound at 37°C under shaking, cultures were subjected to serial 10-fold dilutions (up to 10^6) by adding 20 μl of sample to 180 μl saline (0.85% NaCl). Cell counts were determined using the drop plate method (three 20-μl drops onto LB agar plates). Plates were incubated at 37°C for 16 to 24 h and colonies were counted. Data were obtained from at least two independent experiments performed in triplicate.

Membrane depolarization measurements. Membrane depolarization measurements were performed with 3,3-dipropylthiadicarbocyanine iodide (DiSC3) (5), a lipophilic potentiometric dye that changes its fluorescence intensity in response to changes in transmembrane potential, using *E. coli* strains as described previously (30). An aliquot (180 μl) of the bacterial suspension was placed in a 96-well plate after allowing the dye signal to stabilize for about 5 min, and 20 μl of a solution containing OAK, erythromycin, or their combination was added to obtain the desired final concentration. The fluorescence signal was monitored continuously using a Tecan GENios microplate reader (excitation, 622 nm; emission, 670 nm).

EtBr uptake. Cells were grown overnight in LB broth at 37°C to an optical density at 620 nm of 1.0, washed twice in 200 μl phosphate-buffered saline (PBS), and resuspended in the same buffer containing 0.5% glucose (1 ml). After an incubation of 10 min at 37°C, samples were placed into a 96-well plate and mixed with the test compound containing ethidium bromide (EtBr; final concentration, 1.0 μg/ml). Fluorescence was recorded with a Tecan GENios microplate reader (excitation, 535 nm; emission, 590 nm).

DSC. Differential scanning calorimetry (DSC) measurements were made in a Nano II differential scanning calorimeter (Calorimeter Sciences Corp., Lindon, UT). Lipid films were hydrated at room temperature with peptide solutions in PIPES buffer (20 mM PIPES, 140 mM NaCl, 1 mM EDTA, pH 7.4) or with PIPES buffer alone, vortexed vigorously to make multilamellar vesicles, and then degassed before loading into the sample cell of the calorimeter. Controls using peptide solutions in the sample cell in the absence of lipid showed no transition. Degassed PIPES buffer was placed in the reference cell. The concentration of phospholipids in the samples was maintained at 2.5 mg/ml, and the lipid-to-peptide molar ratio was maintained at 10. The cell volume was 0.34 ml. Samples were equilibrated in the calorimeter at 0°C, and successive heating and cooling scans were carried out at a scan rate of 1.0°C/min with a delay of 5 min between sequential scans in a series to allow thermal equilibration. The resulting curves were analyzed by using the fitting program provided by Microcal Inc. (Northampton, MA) and plotted with the program Origin (version 7.0).

ITC. Titrations were performed in a VP-ITC isothermal titration calorimeter (MicroCal Inc., Northampton, MA) at 30°C. Peptide solutions were placed in the syringe in 10 mM HEPES buffer, 0.14 M NaCl, pH 7.4. Lipopolysaccharide (LPS) or lipoteichoic acid (LTA) at a concentration of 400 μg/ml in 10 mM HEPES, 0.14 M NaCl, pH 7.4, was titrated with 5-μl injections of peptide for LPS or 10-μl injections of peptide for LTA at 30°C. A quantitative thermodynamic analysis of the LPS and LTA titrations was not carried out because of the high degree of heterogeneity of the sugar chains in LPS and LTA. Data were analyzed with the program Origin (version 7.0).

Cytotoxicity assays. Hemoglobin leakage was determined after 1 h incubation in PBS at 37°C using a 10% hematocrit (24). Hemolytic activity data were obtained from at least two independent experiments. In addition, cytotoxicity against human foreskin fibroblasts (HFFs) was assessed using a commercial 2,3-bis-(2-methoxy-4-nitro-5-sulfophenyl)-2*H*-tetrazolium-5-carboxanilide inner salt (XTT) reduction assay kit (Cell Proliferation XTT kit; Biological Industries Ltd., Kibbutz Beit Haemek, Israel). Briefly, 5×10^4 HFFs were seeded onto 96-well plates and incubated for 24 h. Thereafter, the culture medium (Dulbecco modified Eagle medium, 10% fetal bovine serum, antibiotics) was replaced with a series of increasing concentrations of the test compound dissolved in fresh medium. After another 3 h of incubation, XTT reaction solution was added (50 μl XTT/100 μl culture medium), and then the optical density was measured at 450 nm by an enzyme-linked immunosorbent assay plate reader after 2 h of incubation. Cytotoxicity was determined relative to a control having no added OAK.

RESULTS

Biophysical characterization studies of α_{12}-5α_{10}. Table 1 summarizes the MIC values obtained for α_{12}-5α_{10} against a panel of about 50 strains, including GNB and Gram-positive bacteria (GPB). The OAK displayed inhibitory activity against most GNB tested, as evidenced by low MIC values (MIC_{90}, 11.6 μg/ml, cor-

TABLE 1 MICs of α_{12}-5α_{10} against a panel of bacterial strains

Strain	No. of strains	MIC range (μg/ml)
Gram-negative bacteria		
Escherichia coli	22	5.8–11.6
Pseudomonas aeruginosa	9	5.8–11.6
Klebsiella pneumonia	3	5.8–46
Salmonella enterica serovar Typhimurium	1	11.6
Salmonella enterica	1	11.6
Gram-positive bacteria		
Staphylococcus aureus	7	>90
Staphylococcus xylosus	1	46
Staphylococcus epidermidis	1	2.9
Streptococcus bovis	1	>90
Streptococcus agalactiae	1	46
Streptococcus pyogenes	1	5.8
Enterococcus faecalis	1	>90
Enterococcus faecium	1	23
Bacillus cereus	1	>90

responding to 6.2 μM), whereas MIC values against GPB were often significantly higher, albeit a few exceptions were observed (e.g., *Staphylococcus epidermidis* and *Streptococcus pyogenes*). As shown in Fig. 2, no dose-dependent cytotoxicity was associated with α_{12}-5α_{10} against human erythrocytes or skin fibroblasts, at least up to ~100 μg/ml (50 μM). The sequence specificity of these activities was provided by a closely related derivative (C_{12}K-5α_{10}), demonstrating that when the N-terminal amino group was removed, the resulting sequence was nearly devoid of activity against most bacteria (i.e., MICs > 90 μg/ml; data not shown) and was cytotoxic to both erythrocytes and HFFs (Fig. 2), as is often observed with excessively hydrophobic OAKs (13) and HDPs (15, 26). Indeed, C_{12}K-5α_{10} displayed a higher elution time in HPLC than α_{12}-5α_{10} (50.2 versus 41.5 min) and lower solubility in PBS (critical aggregation concentration, 18 versus >180 μg/ml).

The antibacterial mechanism of action was investigated using three different strains of *E. coli*. We first assessed the OAK's ability to affect cell permeability. Figure 3 shows a representative outcome indicating that α_{12}-5α_{10} was responsible for a dose-dependent and rapid bacterial permeabilization to ethidium bromide (Fig. 3a) and for concomitant cell membrane depolarization (Fig. 3b) as well as for a reduction of bacterial viability (Fig. 3c), reflecting a rapid bactericidal mode of action (e.g., 2-log-unit reduction

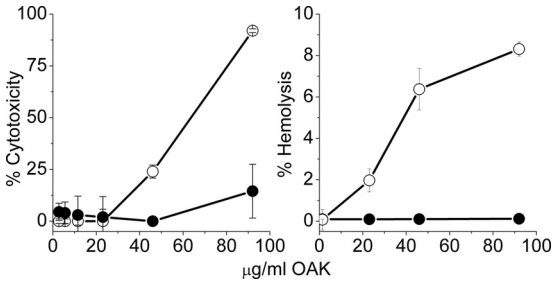

FIG 2 Selectivity of action. (Left) Cytotoxicity of α_{12}-5α_{10} (black circles) and its deaminated analog, C_{12}K-5α_{10} (white circles), assessed using a commercial kit (Cell Proliferation XTT kit) after incubation with 5×10^4 human foreskin fibroblasts (3 h at 37°C); (right) hemolytic activity assessed with human blood (10% hematocrit) after incubation in PBS (1 h at 37°C).

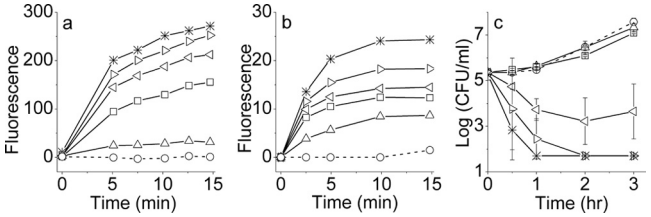

FIG 3 Dose dependence of three kinetic assays performed with *E. coli* 35218: (a) cell permeabilization assessed by EtBr accumulation; (b) cell membrane depolarization assessed by the potential sensitive dye DiSC3 (5); (c) bacterial growth kinetics assessed by CFU count. Symbols: circles, untreated controls; triangles, squares, right triangles, left triangles, and stars, increasing concentrations of α_{12}-5α_{10} (1.4, 2.9, 5.8, 11.5, and 23 μg/ml, respectively). Error bars represent means ± standard deviations.

within 60 and 30 min at 1 and 4 MIC multiples, respectively). A very similar outcome was obtained using two additional *E. coli* strains (14182 and 16327; data not shown).

The OAK's potential for perturbing the membrane structure of GNB was studied by DSC using phospholipid vesicles whose composition (1-palmitoyl-2-oleoyl phosphatidylethanolamine [POPE] and tetraoleoyl cardiolipin [TOCL], 3:1) is believed to mimic the inner membranes of many GNB. The presence of α_{12}-5α_{10} causes a shift in the phase transition of the lipid mixture toward that of the pure POPE component; this shift persists in the cooling scans, indicating that the cationic peptide strongly clusters the anionic lipid TOCL (whose phase transition is below 0), freeing some of the zwitterionic component. This is illustrated in Fig. S1 in the supplemental material. To examine the molecular basis for the observed selective activity against GNB, we next investigated the binding properties to LPS and LTA using ITC. As shown in Fig. S2 in the supplemental material, α_{12}-5α_{10} displayed a higher affinity for LTA than for LPS. Of note is the fact that the opposite was observed with C_{12}K-3β_{10} (8), as further elaborated in Discussion.

Drug combination studies. Figure 4a summarizes data obtained upon exposure of bacteria to various combinations of OAK with erythromycin. The data support the occurrence of a mutually synergistic activity where the presence of sub-MIC levels of each drug significantly sensitized bacteria to the effect of the other drug. For instance, in the presence of 1/4 MIC of α_{12}-5α_{10}, the MIC of erythromycin was reduced by 16-fold (from 128 to 8 μg/ml), whereas in the presence of 1/4 MIC of erythromycin, the MIC of α_{12}-5α_{10} was reduced by 4-fold. An essentially similar outcome was observed with two additional strains (14182 and 16327; data not shown).

To delineate the individual roles played by each compound, we conducted kinetic experiments performed under some of the conditions shown in Fig. 4. Figure 4b shows that at 1/4 MIC, neither compound was efficient in limiting bacterial viability; only their combination has achieved this effect. However, the fact that the resulting effect was bacteriostatic (i.e., no reduction in CFU count), as expected from erythromycin, argues against the direct implication of α_{12}-5α_{10} in this effect, possibly due to its low concentration (2.9 μg/ml or 1/4 MIC). Remarkably, despite the lack of a bactericidal effect, bacteria treated with OAK alone or when combined with erythromycin were subject to rapid depolarization (Fig. 4c) and became permeable to ethidium bromide (Fig. 4d), reaching a maximum within minutes. This finding suggested a

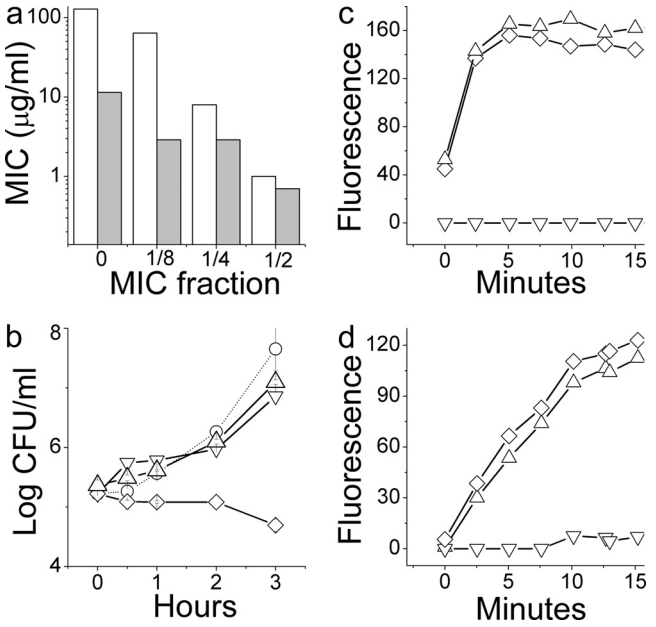

FIG 4 Synergy and its molecular basis assessed against a representative *E. coli* strain. (a) Evolution of erythromycin's MIC values when determined in the presence of a sub-MIC of OAK (white bars) or OAK MIC values in the presence of a sub-MIC of erythromycin (gray bars). (b to d) Assessment of a representative set of synergistic conditions, i.e., 2.9 μg/ml α_{12}-5α_{10} (triangle), 16 μg/ml erythromycin (inverted triangle), and their combination (diamond) performed to determine growth kinetics (b), depolarization (c), and permeabilization (d) of strain 35218.

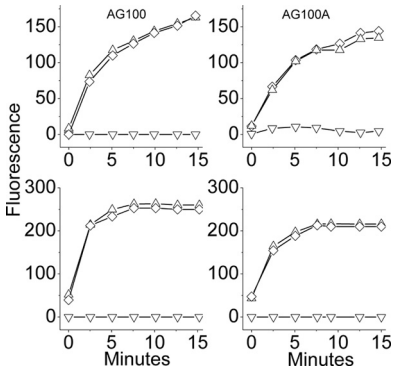

FIG 5 Mechanistic studies using an isogenic pair of *E. coli* strains: *acrAB*-deletion mutant AG100A and wild-type strain AG100. (Top) Cell permeability to ethidium bromide; (bottom) membrane depolarization in these strains at concentrations of 2.9 μg/ml OAK (triangle) and 16 μg/ml erythromycin (inverted triangle) and with their combination (diamond).

potential connection between the sublethal OAK concentration and the synergistic outcome. We therefore investigated the involvement of resistance-nodulation-cell division (RND) pumps using an isogenic pair of *E. coli* strains: the *acrAB*-deletion mutant AG100A and wild-type strain AG100. The MIC value of erythromycin for the wild type was 32-fold higher than that for the deletion mutant, i.e., 128 versus 4 μg/ml, respectively, which is interpreted to reflect normal antibiotic efflux, whereas the OAK displayed only a 2-fold difference, i.e., from 11.5 to 5.8 μg/ml (data not shown). Accordingly, only the wild type was sensitized to erythromycin in the presence of α_{12}-5α_{10}; i.e., the MIC dropped from 128 to 16 μg/ml. Figure 5 shows that under these sublethal conditions the OAK was responsible for depolarization and for permeabilization of both strains.

DISCUSSION

We describe the antibacterial properties of a new OAK derivative whose sequence was responsible for preferential bactericidal activity against GNB. Compared with data published in the literature, there is an interesting structure-activity relationship that emerged. A wide range of studies have established the fact that charge and hydrophobicity attributes represent crucial features of HDPs making major contributions to their multiple biological activities, including target cell specificity. Furthermore, although their specific role in various potency or selectivity aspects is not fully understood, these attributes have long been instrumental in optimization of *de novo* designed chemical mimics of HDPs (9). In this respect, comparison of the properties of analogous sequences such as α_{12}-5α_{10} and C_{12}K-3β_{10} is useful, owing to the exquisite compositional simplicity of these compounds. The main structural feature that distinguishes these analogs is that their charge is spread differently over the peptide backbone (8) (Fig. 1). The data thus provide solid evidence for the significant role of charge distribution in selectivity between GPB and GNB. Although further studies are required for establishing exactly how, we nevertheless demonstrate that α_{12}-5α_{10} has the ability to induce clustering of anionic from zwitterionic lipids and this property can contribute to its antimicrobial activity. The optimal spatial distance between the cationic groups in the β-OAK design for GPB appears to differ from that for GNB. This may be linked to a differential interaction with cell wall components of these bacterial species since, compared with the broad-spectrum C_{12}K-3β_{10}, α_{12}-5α_{10} exhibited a weaker affinity for LPS and a higher affinity for LTA (see Fig. S1 in the supplemental material). The combined data suggest that because of its strong interaction with the LTA layer, α_{12}-5α_{10} is unable to reach the plasma membrane and affect the viability of GPB.

Another interesting finding of this study pertains to the fact that sub-MIC values of α_{12}-5α_{10} have induced rapid membrane depolarization and concomitantly increased cell permeability to EtBr, thereby suggesting that OAK at sub-MICs might allow other similarly small molecules to permeate bacteria. This observation provided the impetus to investigate the potential consequences on RND pumps, which depend on the proton motive force as the energy source for extruding out a variety of molecules, including antibiotics, from the periplasmic space (16, 21). Accordingly, antibiotics such as erythromycin, which are known substrates of the AcrAB-TolC efflux system of *E. coli* (29), are normally prevented from intracellular accumulation and, consequently, are inefficient against GNB. Our data suggest that in the presence of OAK at sub-MIC levels, erythromycin gains access to its ribosomal target due to an impaired efflux function. Various lines of evidence seem to substantiate this hypothesis. (i) Significant synergistic activity was observed upon combination of α_{12}-5α_{10} and erythromycin (Fig. 4 and 5), where bacterial sensitivity to erythromycin was significantly enhanced in the presence of OAK at sub-MIC levels. Accordingly, cell viability and permeability experiments have together delineated the individual role played by each drug: erythromycin was directly responsible for the antibacterial activity, whereas the OAK was responsible for cell permeation. For instance, at 1/4 MICs of OAK (2.9 μg/ml) and 16 μg/ml erythromycin, neither compound alone was efficient in limiting bacterial

viability; only their combination achieved this effect (Fig. 4). The observed bacteriostatic outcome (i.e., no reduction in CFU count) implicates erythromycin in this effect since the OAK exerts a bactericidal mode of action. (ii) At these concentrations, bacteria were subject to rapid depolarization (Fig. 2 and 4). The fact that this effect was not altered by the presence of erythromycin (alone or in combination) also argues for the OAK's role in membrane depolarization, whereas erythromycin does not seem to affect membrane polarization. To shed light onto the molecular basis for these observations, we investigated the involvement of RND pumps using an *acrAB*-deletion mutant (AG100A) and compared it with the involvement in its wild-type strain (AG100) (25). Data presented in Fig. 5 indicate that the OAK is not a good substrate of the RND system, unlike erythromycin. Accordingly, only the wild type was sensitized to erythromycin in the presence of α_{12}-$5\alpha_{10}$ (the MIC dropped to a level similar to that for clinical isolates). Moreover, the OAK was responsible for depolarization and for permeation of both strains; however, in AG100A, which is already sensitive to erythromycin, only the erythromycin-resistant bacteria can actually benefit from these effects, as reflected by the reduced MIC value.

The combined data support the view that α_{12}-$5\alpha_{10}$ is able to overcome resistance/insensitivity to erythromycin by depriving bacteria of the transmembrane potential, the energy source needed for AcrAB-TolC function, thereby inhibiting erythromycin efflux. Membrane potential is critical for bacterial cell division, providing the energy required for the correct location/distribution of many division-related protein systems (23). Hence, if a sub-MIC of OAK can dissipate the membrane potential in GNB, this would disrupt a wide range of crucial processes that derive their energy from the proton motive force. This includes the RND efflux system. In fact, inactivation of the *acrAB* operon in GNB was shown to decrease antibiotic MICs by orders of magnitude (10). Collectively, therefore, the data suggest the following scenario: at sub-MICs, relatively few OAK molecules reach the cytoplasmic membrane of GNB, but enough molecules reach the membrane to induce depolarization but not cell death. Membrane depolarization is promoted by an avid interaction with cardiolipin and segregation of anionic and zwitterionic phospholipids, which leads to breaching of the permeability barrier through defects (cracks) in the membrane that allow proton leakage. This, in turn, likely affects the function of multiple membrane protein systems, as exemplified by the AcrAB-TolC efflux system, which leads to increased cell permeability to small molecules. In the absence of erythromycin, this damage is repaired, hence the observed lack of a significant difference in cell viability. However, if erythromycin is present under these conditions, the antibiotic can gain access to the cytoplasm and inhibit ribosomal synthesis.

Notwithstanding these considerations, synergistic activity was also observed upon combination of erythromycin with α_{12}-$5\alpha_{10}$ (Fig. 4a), indicating that bacterial sensitivity to the OAK was significantly enhanced in the presence of a sub-MIC of erythromycin (although to a lower extent). While this aspect remains to be elucidated, it might stem from the cationic character of erythromycin, whose positive charge may contribute to enhancing the charge-based effect of OAK, particularly as this effect is observed at relatively high erythromycin concentrations. It nonetheless seems that this mutual synergism may represent an efficient means for overcoming innate bacterial resistance to erythromycin.

ACKNOWLEDGMENTS

This research was supported by the Israel Science Foundation (grant 283/08 to A.M.) and by the Canadian Institutes of Health Research (grant MOP 86608 to R.M.E.).

REFERENCES

1. **Choi S, et al.** 2009. De novo design and in vivo activity of conformationally restrained antimicrobial arylamide foldamers. Proc. Natl. Acad. Sci. U. S. A. **106**:6968–6973.
2. **Goodman CM, Choi S, Shandler S, DeGrado WF.** 2007. Foldamers as versatile frameworks for the design and evolution of function. Nat. Chem. Biol. **3**:252–262.
3. **Hancock RE, Sahl HG.** 2006. Antimicrobial and host-defense peptides as new anti-infective therapeutic strategies. Nat. Biotechnol. **24**:1551–1557.
4. **Held-Kuznetsov V, Rotem S, Assaraf YG, Mor A.** 2009. Host-defense peptide mimicry for novel antitumor agents. FASEB J. **23**:4299–4307.
5. **Kuroda K, DeGrado WF.** 2005. Amphiphilic polymethacrylate derivatives as antimicrobial agents. J. Am. Chem. Soc. **127**:4128–4129.
6. **Liu D, DeGrado WF.** 2001. De novo design, synthesis, and characterization of antimicrobial beta-peptides. J. Am. Chem. Soc. **123**:7553–7559.
7. **Livne L, Epand RF, Papahadjopoulos-Sternberg B, Epand RM, Mor A.** 2010. OAK-based cochleates as a novel approach to overcome multidrug resistance in bacteria. FASEB J. **24**:5092–5101.
8. **Livne L, et al.** 2009. Design and characterization of a broad-spectrum bactericidal acyl-lysyl oligomer. Chem. Biol. **16**:1250–1258.
9. **Mor A.** 2010. Chemical mimics with systemic efficacy, 1st ed. CABI Publishing, Wallingford, Oxfordshire, United Kingdom.
10. **Nikaido H.** 1998. Antibiotic resistance caused by gram-negative multidrug efflux pumps. Clin. Infect. Dis. **27**(Suppl 1):S32–S41.
11. **Patch JA, Barron AE.** 2003. Helical peptoid mimics of magainin-2 amide. J. Am. Chem. Soc. **125**:12092–12093.
12. **Porter EA, Wang X, Lee HS, Weisblum B, Gellman SH.** 2000. Non-haemolytic beta-amino-acid oligomers. Nature **404**:565.
13. **Radzishevsky IS, et al.** 2008. Structure-activity relationships of antibacterial acyl-lysine oligomers. Chem. Biol. **15**:354–362.
14. **Radzishevsky IS, et al.** 2007. Improved antimicrobial peptides based on acyl-lysine oligomers. Nat. Biotechnol. **25**:657–659.
15. **Radzishevsky IS, et al.** 2005. Effects of acyl versus aminoacyl conjugation on the properties of antimicrobial peptides. Antimicrob. Agents Chemother. **49**:2412–2420.
16. **Rieg S, Huth A, Kalbacher H, Kern WV.** 2009. Resistance against antimicrobial peptides is independent of Escherichia coli AcrAB, Pseudomonas aeruginosa MexAB and Staphylococcus aureus NorA efflux pumps. Int. J. Antimicrob. Agents **33**:174–176.
17. **Rotem S, et al.** 2008. Analogous oligo-acyl-lysines with distinct antibacterial mechanisms. FASEB J. **22**:2652–2661.
18. **Sarig H, Goldfeder Y, Rotem S, Mor A.** 2011. Mechanisms mediating bactericidal properties and conditions that enhance the potency of a broad-spectrum oligo-acyl-lysyl. Antimicrob. Agents Chemother. **55**:688–695.
19. **Sarig H, et al.** 2010. A miniature mimic of host defense peptides with systemic antibacterial efficacy. FASEB J. **24**:1904–1913.
20. **Sarig H, Ohana D, Epand RF, Mor A, Epand RM.** 2011. Functional studies of cochleate assemblies of an oligo-acyl-lysyl with lipid mixtures for combating bacterial multidrug resistance. FASEB J. **25**:3336–3343.
21. **Schumacher A, et al.** 2007. Intracellular accumulation of linezolid in Escherichia coli, Citrobacter freundii and Enterobacter aerogenes: role of enhanced efflux pump activity and inactivation. J. Antimicrob. Chemother. **59**:1261–1264.
22. **Srinivas N, et al.** 2010. Peptidomimetic antibiotics target outer-membrane biogenesis in Pseudomonas aeruginosa. Science **327**:1010–1013.
23. **Strahl H, Hamoen LW.** 2010. Membrane potential is important for bacterial cell division. Proc. Natl. Acad. Sci. U. S. A. **107**:12281–12286.
24. **Tossi A, et al.** 1997. An approach combining rapid cDNA amplification and chemical synthesis for the identification of novel, cathelicidin-derived, antimicrobial peptides. Methods Mol. Biol. **78**:133–150.
25. **Wolfart K, et al.** 2006. Synergistic interaction between proton pump inhibitors and resistance modifiers: promoting effects of antibiotics and plasmid curing. In Vivo **20**:367–372.
26. **Yin LM, Li EMJ, Yip CM, Deber CM.** 2012. Roles of hydrophobicity and

charge distribution of cationic antimicrobial peptides in peptide-membrane interactions. J. Biol. Chem. **287**:7738–7745.
27. **Zaknoon F, et al.** 2011. Antiplasmodial properties of acyl-lysyl oligomers in culture and animal models of malaria. Antimicrob. Agents Chemother. **55**:3803–3811.
28. **Zasloff M.** 2002. Antimicrobial peptides of multicellular organisms. Nature **415**:389–395.
29. **Zgurskaya HI, Nikaido H.** 1999. Bypassing the periplasm: reconstitution of the AcrAB multidrug efflux pump of Escherichia coli. Proc. Natl. Acad. Sci. U. S. A. **96**:7190–7195.
30. **Zhang L, Dhillon P, Yan H, Farmer S, Hancock RE.** 2000. Interactions of bacterial cationic peptide antibiotics with outer and cytoplasmic membranes of Pseudomonas aeruginosa. Antimicrob. Agents Chemother. **44**:3317–3321.